 CMES, vol.36, no.3, pp.193-212, 2008

Probabilistic Collocation used in a Two-Step approach for efficient uncertainty quantification in computational fluid dynamics.

G.J.A. Loeven[1,2] **and H. Bijl**[3]

Abstract: In this paper a Two-Step approach is presented for uncertainty quantification for expensive problems with multiple uncertain parameters. Both steps are performed using the Probabilistic Collocation method. The first step consists of a sensitivity analysis to identify the most important parameters of the problem. The sensitivity derivatives are obtained using a first or second order Probabilistic Collocation approximation. For the most important parameters the probability distribution functions are propagated using the Probabilistic Collocation method using higher order approximations. The Two-Step approach is demonstrated for flow around a NACA0012 airfoil with eight uncertain parameters in the free stream conditions and geometry. The first step identified the freestream velocity, angle of attack, and the camber of the airfoil as the three most important parameters. In the second step the probability distributions of all three parameters are propagated using higher order Probabilistic Collocation approximations. Statistical properties of the lift and drag are obtained, as well as uncertainty bounds for the pressure and skinfriction on the surface of the airfoil.

Keyword: Probabilistic Collocation, Polynomial Chaos, Computational Fluid Dynamics, Uncertainty Quantification, Sensitivity Analysis.

1 Introduction

Interest in uncertainty quantification for computational fluid dynamic problems is growing rapidly. Due to efficient algorithms and increasing computing power, uncertainty quantification has become feasible for computationally intensive prob-

[1] Ph. D. researcher, Faculty of Aerospace Engineering, P.O. Box 5058, 2600 GB Delft, The Netherlands.

[2] Corresponding author: G.J.A.Loeven@TUDelft.nl

[3] Full Professor, Faculty of Aerospace Engineering, P.O. Box 5058, 2600 GB Delft, The Netherlands.

lems. In Computational Fluid Dynamics (CFD) problems uncertainties are inherently present due to physical variations in the geometry and flow conditions. One can think of atmospheric conditions and production tolerances in the fabrication process.

If deterministic computations are computationally intensive, efficient uncertainty quantification methods are required. Extensive research has been performed on the use polynomial chaos methods. The polynomial chaos methods are based on the homogeneous chaos theory of Wiener (1938). To obtain the coefficients of the polynomial chaos expansion, the equations can be solved by applying the stochastic Galerkin method [Babuška, Nobile, Zouraris, and Tempone (2004); Ghanem and Spanos (1991); Xiu and Karniadakis (2002); Xiu, Lucor, Su, and Karniadakis (2002)]. This approach results in a set of coupled equations, which means that the source code of the CFD solver should be available for implementation.

To be able to use a commercial CFD solver, a so-called non-intrusive method is used in this paper. Non-intrusive methods use the deterministic solver as a black-box for uncertainty propagation [Loeven, Witteveen, and Bijl (2007); Hosder, Walters, and Perez (2006); Parussini and Pediroda (2007, 2008); Reagan, Najm, Ghanem, and Knio (2003)]. The Probabilistic Collocation method [Babuška, Nobile, and Tempone (2007); Loeven, Witteveen, and Bijl (2007); Tatang, Pan, Prinn, and McRae (1997)] is employed, since it converges exponentially with respect to the polynomial order for arbitrary input distributions. The method is also based on the polynomial chaos expansion, only here the coefficients are obtained using Gauss quadrature. This results in a decoupled set of equations.

A disadvantage of the standard Probabilistic Collocation method is the curse of dimensionality. For multiple uncertain parameters, for CFD above say five, even low order approximations cannot be computed within reasonable time. A solution to this problem can be sparse grid approaches [Ganapathysubramanian and Zabaras (2007); Xiu and Hesthaven (2005)]. Advantages of sparse grid approaches are the fact that all uncertain parameters can be propagated efficiently and combined effects of the parameters are computed. However, some uncertain parameters may not affect the solution much, so taking them into account results in additional computations that do not contribute to the stochastic solution of interest.

In this paper a Two-Step approach is followed by first performing a sensitivity analysis and secondly propagating the statistics of the most important parameter(s) in the next step. The sensitivity analysis is based on the scaled sensitivity derivatives [Turgeon, Pelletier, and Borggaard (2003)]. The sensitivity derivatives are obtained from a first or second order Probabilistic Collocation approximation, depending on the distribution of the uncertain parameters. For each output of interest, the scaled sensitivity derivatives are compared, yielding the most important parameters. Next

the probability distribution functions are propagated using higher order Probabilistic Collocation approximations. The Two-Step approach starts with a sensitivity analysis based on separate effects of the uncertain parameters, so interactions between parameters are not taken into account in this step. The second step is performed using a multidimensional Probabilistic Collocation expansion to include interactions between the parameters. By taking into account only the most important parameters, the number of deterministic computations is reduced significantly.

This paper starts with explaining the Two-Step approach in section 2. Where first the Probabilistic Collocation method in section 2.1 and secondly the sensitivity analysis using the scaled sensitivity derivatives in section 2.2 are shown. The Two-Step approach is then applied to flow around a NACA0012 airfoil with eight uncertain parameters in section 3. The paper is concluded in section 4.

2 Two-Step approach for expensive problems with multiple uncertain parameters

Since the propagation of probability distributions for multiple uncertain parameters is computationally intensive a Two-Step approach is followed. The first step consists of a sensitivity analysis using scaled sensitivity derivatives [Turgeon, Pelletier, and Borggaard (2003)], which is performed to identify the most important parameter of the problem. After that in the second step the uncertainty of the identified parameter is propagated using the Probabilistic Collocation method [Babuška, Nobile, and Tempone (2007); Loeven, Witteveen, and Bijl (2007); Tatang, Pan, Prinn, and McRae (1997)] which results in the stochastic response of the solution based on the input distribution of the uncertain parameter. The Probabilistic Collocation method is a polynomial chaos type method [Ghanem and Spanos (1991); Wiener (1938)], which is non-intrusive, it uses a deterministic solver as a black-box. For a low number of uncertain parameters, the method is more efficient than the intrusive Galerkin Polynomial Chaos method and other non-intrusive methods [Loeven, Witteveen, and Bijl (2006, 2007)]. The sensitivity analysis is based on separate effects of each parameter. The full Probabilistic Collocation computations also includes interaction between the uncertain parameters.

2.1 The Probabilistic Collocation Method

In the Probabilistic Collocation method a polynomial chaos expansion is constructed based on Lagrange polynomials. Secondly, Gauss quadrature weighted by the probability density function of the uncertain parameter is used to compute the Galerkin projection and to integrate the approximation of the distribution function. By using Gauss quadrature a decoupled set of equations is obtained and the approximated distribution is integrated exactly to obtain the mean and variance.

Probabilistic Collocation expansion

The solution and each variable depending on the uncertain input parameter is expanded as follows:

$$u(\mathbf{x},t,\omega) = \sum_{i=1}^{N_p} u_i(\mathbf{x},t) h_i(\xi(\omega)), \tag{1}$$

where the solution $u(\mathbf{x},t,\omega)$ is a function of space $\mathbf{x}$ and time t and the random event $\omega \in \Omega$, and the number of collocation points N_p. The complete probability space is given by $(\Omega, \mathscr{F}, P)$, with Ω the set of outcomes, $\mathscr{F} \subset 2^\Omega$ the σ-algebra of events and $P : \mathscr{F} \to [0,1]$ a probability measure. Furthermore, $u_i(\mathbf{x},t)$ is the solution $u(\mathbf{x},t,\omega)$ at the collocation point ω_i; h_i is the Lagrange interpolating polynomial chaos corresponding to the collocation point ω_i; ξ is the random basis. The Lagrange interpolation results in polynomial chaoses. A polynomial chaos is a polynomial of random variables instead of ordinary variables. The term chaos in this context originates from the paper of Wiener (1938) on homogeneous chaos, and should not be confused with deterministic chaos of dynamical systems. The Lagrange interpolating polynomial is a function in terms of the random variable $\xi(\omega)$, which is chosen such that the uncertain input parameter is a linear transformation of $\xi(\omega)$. The Lagrange interpolating polynomial chaos is the polynomial chaos $h_i(\xi(\omega))$ that passes through the N_p collocation points, with $h_i(\xi(\omega_j)) = \delta_{ij}$. The collocation points are chosen such that they correspond to the Gauss quadrature points used to integrate the function $u(\mathbf{x},t,\omega)$ in the ω domain. For convenience of notation the argument ω is omitted from here on. The solution is integrated to obtain the mean or variance. When multiple uncertain parameters are present, the collocation points are obtained from tensor products of one dimensional points. The number of collocation points N_p then becomes $N_p = (P+1)^d$, where P is the order of approximation and d then dimension of the stochastic problem (i.e. number of uncertain parameters). To find the suitable Gauss quadrature points and weights the procedure below is followed.

Computing Gaussian quadrature points with corresponding weights

A powerful method to compute Gaussian quadrature rules is by means of the Golub-Welsch algorithm [Golub and Welsch (1969)]. This algorithm requires the recurrence coefficients [Gautschi (2005)] of polynomials which are orthogonal with respect to the weighting function of the integration. Exponential convergence for arbitrary probability distributions is obtained when the polynomials are orthogonal with respect to the probability density function of ξ, so $w(\xi) = f_\xi(\xi)$. The Golub-Welsch algorithm requires the recurrence coefficients of the orthogonal polynomi-

als. The recurrence coefficients are computed using the discretized Stieltjes procedure [Gander and Karp (2001)], which is a stable method for arbitrary distribution functions. Orthogonal polynomials satisfy the following three-term recurrence relation:

$$\begin{aligned} \Psi_{i+1}(\xi) &= (\xi - \alpha_i)\Psi_i(\xi) - \beta_i \Psi_{i-1} \qquad i = 1,2,\ldots,N_p, \\ \Psi_0(\xi) &= 0,\ \Psi_1(\xi) = 1, \end{aligned} \tag{2}$$

where α_i and β_i are the recurrence coefficients determined by the weighting function $w(\xi)$ and $\{\Psi_i(\xi)\}_{i=1}^{N_p}$ is a set of (monic) orthogonal polynomials with $\Psi_i(\xi) = \xi^i + \mathcal{O}(\xi^{i-1}), i = 1,2,\ldots,N_p$. The recurrence coefficients are given by the Darboux's formulae [Gautschi (2005)]:

$$\begin{aligned} \alpha_i &= \frac{(\xi\Psi_i, \Psi_i)}{(\Psi_i, \Psi_i)} \qquad i = 1,2,\ldots,N_p, \\ \beta_i &= \frac{(\Psi_i, \Psi_i)}{(\Psi_{i-1}, \Psi_{i-1})} \qquad i = 2,3,\ldots,N_p, \end{aligned} \tag{3}$$

where $(\cdot,\cdot)$ denotes an inner product. The first coefficient β_1 is given by (Ψ_1, Ψ_1). Gander and Karp (2001) showed that discretizing the weighting function leads to a stable algorithm. Therefore the discretized Stieltjes procedure is used to obtain the recurrence coefficients. Hereto, first the weighting function $w(\xi)$ is discretized by

$$w_N(\xi) = \sum_{j=1}^{N} w_j \delta(\xi - \xi_j), \qquad w_j > 0, \tag{4}$$

where δ is the Dirac delta function. Stieltjes' procedure starts with $i = 1$. With Eq. (3) the first coefficient α_1 is computed, $\beta_1 = \sum_{j=1}^{N} w_j$. Now $\Psi_2(\xi)$ is computed by Eq. (2) using α_1 and β_1. This is repeated for $i = 2,3,\ldots,N_p$. When continuous weighting functions are considered $N_p \ll N$, for discrete measures $N_p \leq N$. The inner product is defined as

$$(p(\xi), q(\xi)) = \int_S p(\xi) q(\xi) w_N(\xi) \mathrm{d}\xi = \sum_{j=1}^{N} w_j p(\xi_j) q(\xi_j), \tag{5}$$

for two functions $p(\xi)$ and $q(\xi)$.

From the recurrence coefficients α_i and β_i, $i = 1,2,\ldots,N_p$, the collocation points ξ_i and corresponding weights w_i are computed using the Golub-Welsch algorithm [Golub and Welsch (1969)]. With the recurrence coefficients the following matrix

is constructed:

$$J = \begin{bmatrix} \alpha_1 & \sqrt{\beta_2} & & & & \\ \sqrt{\beta_2} & \alpha_2 & \sqrt{\beta_3} & & \emptyset & \\ & \sqrt{\beta_3} & \alpha_3 & \sqrt{\beta_4} & & \\ & & \ddots & \ddots & \ddots & \\ & \emptyset & & \sqrt{\beta_{N_p-1}} & \alpha_{N_p-1} & \sqrt{\beta_{N_p}} \\ & & & & \sqrt{\beta_{N_p}} & \alpha_{N_p} \end{bmatrix}. \tag{6}$$

The eigenvalues of J are the collocation points ξ_i, $i = 1,\ldots,N_p$, which are the roots of the polynomial of order N_p from the set of the constructed orthogonal polynomials. The weights are found by $w_i = \beta_1 v_{1,i}^2$, $i = 1,\ldots,N_p$, where $v_{1,i}$ is the first component of the normalized eigenvector corresponding to eigenvalue ξ_i.

Now the collocation points ξ_i in the ξ-domain are known. They are mapped to the ω-domain using the distribution function of ξ. The collocation points ω_i are found by

$$\omega_i = F_\xi(\xi_i), \qquad i = 1,\ldots,N_p. \tag{7}$$

If multiple uncertain parameters are present, the collocation points are found using tensor products of one dimensional points or using a sparse grid approach [Ganapathysubramanian and Zabaras (2007); Xiu and Hesthaven (2005)].

Application to a general model

The application of Probabilistic Collocation method to a general model is shown. The model is a black box and can be for example a CFD solver. It is demonstrated how the method is used when the parameter of interest is a functional of the solution, like the lift of an airfoil. Expansion (1) is substituted into the model, represented here by the operator $\mathscr{L}$, which depends on an uncertain input parameter $a(\omega)$:

$$\mathscr{L}(a(\omega))\, u(\mathbf{x},t,\omega) = S(\mathbf{x},t). \tag{8}$$

A Galerkin projection on each basis $\{h_k(\xi(\omega))\}$ is applied:

$$\left(\mathscr{L}(a(\omega)) \sum_{i=1}^{N_\mathrm{p}} u_i(\mathbf{x},t) h_i, h_k\right) = (S, h_k), \qquad k = 1,\ldots,N_\mathrm{p}. \tag{9}$$

This projection is approximated using Gaussian quadrature as in Eq. (5), with collocation points and corresponding weights based on the input distribution. The result is a fully decoupled system of equations, similar to the deterministic Eq. (8):

$$\mathscr{L}(a(\omega_k))u_k(\mathbf{x},t) = S(\mathbf{x},t), \qquad k = 1,\ldots,N_\mathrm{p}. \tag{10}$$

The distribution function is obtained from Eq. (1). From the distribution one can extract the probability density function or confidence intervals. The mean and variance of the solution are found by

$$\mu_u = \sum_{i=1}^{N_\mathrm{p}} u_i(\mathbf{x},t)w_i, \tag{11}$$

$$\sigma_u^2 = \sum_{i=1}^{N_\mathrm{p}} (u_i(\mathbf{x},t))^2 w_i - \left(\sum_{i=1}^{N_\mathrm{p}} u_i(\mathbf{x},t)w_i\right)^2, \tag{12}$$

where w_i are the weights corresponding to the collocation points ω_i. These relations are derived from the definition of the mean and variance.

Output of interest

Often the output of interest is a functional of the solution, like the lift force of an airfoil. The flow around the airfoil is computed and integration of the pressure on the surface of the airfoil yields the lift. Due to the uncertainty present in the system, the lift becomes a random variable as well. The lift is written as a Probabilistic Collocation expansion as follows

$$L = \sum_{i=1}^{N_p} L_i(t)h_i(\xi), \tag{13}$$

where $L_i(t)$ is the lift force at time t for collocation point ω_i. $L_i(t)$ follows from the deterministic computations for every collocation point. The distribution function of the lift L is then constructed using Eq. (13), the mean and variance are obtained using Eqs. (11) and (12). For the Galerkin Polynomial Chaos method the functionals have to be applied to the reconstructed solution $u(\mathbf{x},t,\omega)$, which can give troubles [Loeven, Sarkar, Witteveen, and Bijl (2007); Sarkar, Witteveen, Loeven, and Bijl (2008)].

A stochastic computation is now performed as follows:

1. *Specify input distributions* for every uncertain parameter by determining the probability density function.

2. *Compute collocation points and weights* based on the probability density functions of the uncertain parameter, using Eqs. (3), (4), (6), and (7).

3. *Perform deterministic computations* for every collocation point. These computations can be performed in parallel.

4. *Construct the stochastic solution* using all obtained deterministic solutions, e.g. mean/variance fields, uncertainty bars or probability density functions, using Eqs. (1), (11), and (12).

2.2 Sensitivity analysis to obtain the most important parameter

Sensitivity analysis is based on the scaled sensitivity derivative [Turgeon, Pelletier, and Borggaard (2003)]. In this paper sensitivity derivatives are used to identify the most important uncertain parameter in a particular physical system. Sensitivity analysis is used here as an efficient way of reducing the amount of uncertain parameters. A reduction of the amount of uncertain parameters results directly in less required deterministic solves and therefore reduces the computational time.

The sensitivity derivative is defined as the partial derivative of the solution $u(\mathbf{x},t,\omega)$ or any output of interest with respect to the uncertain parameter $a(\omega)$. The sensitivity derivatives are computed by differentiating a first or second order PC approximation. One can also use a finite difference approach, but then the size of the difference should be carefully chosen. A smaller difference leads to more accurate sensitivity derivatives, however, truncation errors of the deterministic solver may produce wrong sensitivity derivatives. For symmetric distributions, like the normal distribution, the second collocation point with corresponding solution $u_2(\mathbf{x},t)$ is equal to the computation with deterministic settings. For this case two solves for each parameter are required to obtain the sensitivity derivative, with a total of $2d+1$ solves for the complete sensitivity analysis, with d the number of uncertain parameters. For asymmetric distributions $3d$ deterministic solves would be required. Therefore, to save computational costs, a first order Probabilistic Collocation expansion is used for cases with asymmetric distributions, requiring $2d$ solves. In this paper truncated normal distributions are used, which are symmetric. The approximation of the derivative is then obtained by first differentiating Eq. (1)

for $N_p = 3$ with respect to $\xi(\omega)$:

$$\left.\frac{\partial u}{\partial \xi}\right|_a = u_{1,a}(\mathbf{x},t)\left[\frac{\xi(\omega_2)-\xi(\omega_3)}{(\xi(\omega_1)-\xi(\omega_2))(\xi(\omega_1)-\xi(\omega_3))}\right] + u_{2,a}(\mathbf{x},t)\left[\frac{2\xi(\omega_2)-\xi(\omega_1)-\xi(\omega_3)}{(\xi(\omega_2)-\xi(\omega_1))(\xi(\omega_2)-\xi(\omega_3))}\right] + u_{3,a}(\mathbf{x},t)\left[\frac{\xi(\omega_2)-\xi(\omega_1)}{(\xi(\omega_3)-\xi(\omega_1))(\xi(\omega_3)-\xi(\omega_2))}\right], \tag{14}$$

where $u_{i,a}(\mathrm{x},t)$ indicates the i^{th} collocation point for uncertain parameter a. The parameter a is a linear combination of the random variable ξ, so $a = A_a\xi + B_a$, with constants A_a and B_a. The sensitivity derivative of the solution with respect to parameter a is given by

$$\frac{\partial u}{\partial a} = \left.\frac{\partial u}{\partial \xi}\right|_a \frac{\partial \xi}{\partial a} = \frac{1}{A_a}\left.\frac{\partial u}{\partial \xi}\right|_a. \tag{15}$$

When more parameters are involved in the problem the scaled sensitivity derivative with respect to each parameter is calculated. One has to take into account that this procedure provides the sensitivity information for each parameters separately, so no combined effects are taken into account in this step. By scaling the sensitivity derivatives with the standard deviation of the parameters a good estimate of the effect of the uncertain parameter on the solution is obtained. If the solution depends on N parameters, the most important parameter is

$$\max\left\{\sigma_{a_1}\frac{\partial u}{\partial a_1},\ \sigma_{a_2}\frac{\partial u}{\partial a_2},\ \ldots,\ \sigma_{a_N}\frac{\partial u}{\partial a_N}\right\}. \tag{16}$$

Once the most important parameter is obtained by Eq. (16) the stochastic response of the solution can be computed based on the input distribution of the uncertain parameter.

3 Two-Step Framework applied to NACA 0012 airfoil with 8 uncertain parameters

In this section the Two-Step framework is applied to steady flow around a NACA0012 airfoil with eight uncertain parameters. A commercial deterministic CFD code is used to compute the deterministic solves for every collocation point. The deterministic case is flow around a NACA0012 airfoil at an angle of attack α of 5 degrees and a free stream velocity U of 100. The Reynolds number is equal to $3 \cdot 10^6$. The deterministic computations are performed using the Fine™/Hexa solver by Numeca

Int. on a grid of approximately 100,000 cells. A close-up of the grid layout is shown in Fig. 1(a). A grid convergence study was performed to make sure the deterministic solutions are fully grid independent. If the deterministic computations are not grid independent or numerically sufficiently converged, the induced errors may be larger than the variations due to the uncertain parameter. For the grid convergence study grids of 50, 75, 100, 125, and 150 thousand cells were used. The grid of 100,000 cells showed no significant difference compared to the finer grids and was used for further computations.

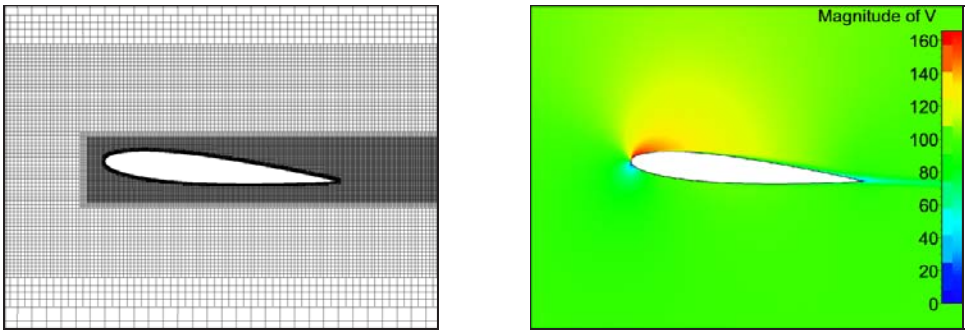

(a) (b)

Figure 1: The mesh layout near the airfoil (a) and magnitude of velocity (b) of the mean conditions.

The flow is modeled by the Reynolds-Averaged Navier-Stokes (RANS) equations using the Spalart-Allmaras turbulence model. Fig. 1(b) shows the magnitude of velocity of the mean conditions. The mean air properties are at 0m ISA. The uncertainties are present in the free stream flow conditions, i.e. the velocity U, angle of attack α, pressure p, temperature T, viscosity ν, and turbulence intensity I and in the geometry by the thickness t and camber c. The free stream conditions are never constant in real flight due to atmospheric irregularities. The geometric uncertainties result from production tolerances in the fabrication process, as a result of which the actual airoil slightly differs from the designed shape.

Input distributions

All uncertain parameters are assumed to have a truncated normal distribution and are shown in Fig. 2; the specifications of the distributions are given in Tab. 1. Truncated normal distributions are used to avoid unphysical settings and too large variations. The variations in the geometry are chosen such that the parameters vary

within a reasonable interval. The parameters of the freestream are based on variations that can occur in flight, due to uncertain height and atmospheric conditions. The kinematic viscosity is varied to see the effect of the Reynolds number. For real life applications the input distributions should be measured to be able to find a realistic input distribution. One can think of measuring the shape of products after production or measuring air properties and freestream velocity and angle of attack during flight. Currently, these data are not available yet, so assumptions on the input distributions have to be made. For the truncated normal distributions it is important to use the orthogonalization procedure described in section 2.1. If one would use the Hermite polynomials (corresponding to a normal distribution), the support is infinite and collocation points will fall outside the truncation interval for higher orders of approximation.

Table 1: Distribution description of the uncertain parameters. All parameters have a truncated normal distributions, truncated on the $\mu \pm 3\sigma$ interval.

Parameter	Mean μ	Standard deviation σ	Minimal value	Maximal value	Coefficient of variation (*COV*)
U	100	5	85	115	5 %
α	5	0.3333	4	6	6.67 %
t	12	0.3333	11	13	2.78 %
c	0	0.16667	-0.5	0.5	-
p	101325	1013.25	98285	104365	1 %
T	288.15	2.8815	279.5	296.8	1 %
ν	$3.3333 \cdot 10^{-5}$	$3.3333 \cdot 10^{-7}$	$3.2333 \cdot 10^{-5}$	$3.4333 \cdot 10^{-5}$	1 %
I	0.1	0.005	0.085	0.115	5 %

To propagate the distributions of all eight parameters for a second order PC approximation requires 6561 deterministic solves. The RANS computation of the NACA0012 airfoil on the grid of 100,000 cells runs in the order of 10 CPU hours on an AMD Opteron 2800 MHz processor. A second order PC approximation is not feasible for this problem for all parameters simultaneously. To be able to perform uncertainty quantification, the Two-Step approach is employed. The sensitivity analysis only requires 17 deterministic solves for all eight parameters. After that only the probability distributions of the most important parameters are propagated.

3.1 Step I: Identifying the most important parameter

In this paper the lift and drag forces and coefficients are considered as the main output of interest. The scaled sensitivity derivatives are shown in Fig. 3 for the lift and drag forces and Fig. 4 for the lift and drag coefficients. The notation of the scaled sensitivities is for example $L_{\tilde{U}} = \sigma_U \partial L / \partial U$ for the scaled sensitivity derivative of

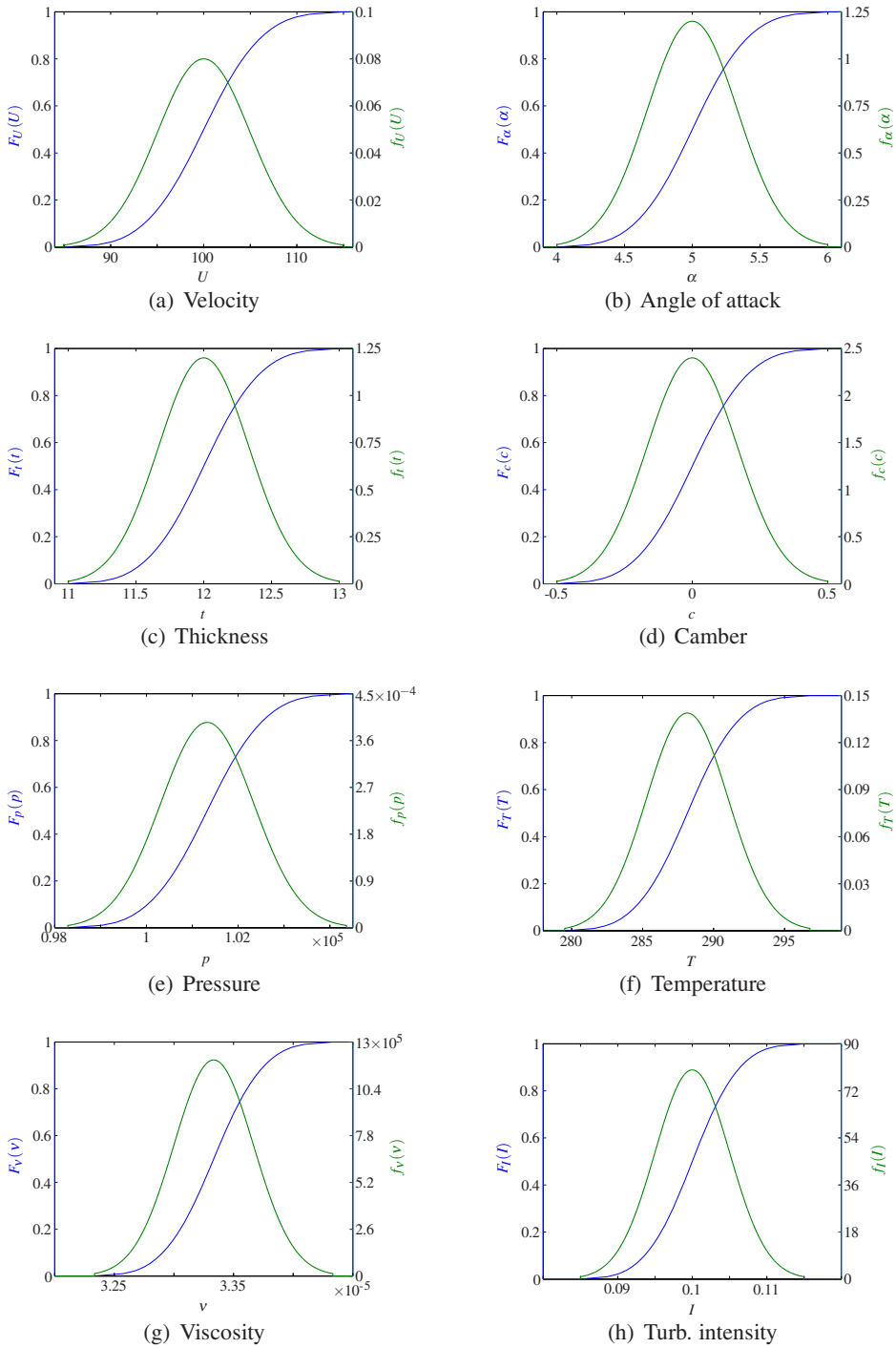

(a) Velocity (b) Angle of attack

(c) Thickness (d) Camber

(e) Pressure (f) Temperature

(g) Viscosity (h) Turb. intensity

Figure 2: Uncertain input parameters; the cumulative distribution functions F are shown by the blue line (–) and the probability density functions f are indicated by the green line (–).

the lift force L with respect to the free stream velocity U. Clearly, the conclusions depend on the output of interest. Furthermore, the sensitivity derivatives show the effects of the parameters separately. The user should, therefore, be careful when selecting the most important parameters, because combined effects are not taken into account in this step. The scaled sensitivity derivatives of the forces in Fig. 3 show expected variations in the order of 10% of the deterministic value. Since the forces depend on the dynamic pressure, the velocity U is most dominant in this case. Also the angle of attack α shows significant variation, as well as the camber c for the lift force. For the coefficients, however, Fig. 4 shows that the expected variations are different. The lift coefficient variations are expected up to 7%, mainly due to an uncertain angle of attack α and camber c. The other parameters are not important for the lift coefficient. The variations of the drag coefficient are about 2.5%, due to uncertain angle of attack α. All other parameters are expected to contribute less than 1% variation in the drag coefficient. Based on these observations, further computations are performed for uncertain velocity U, angle of attack α, and camber c.

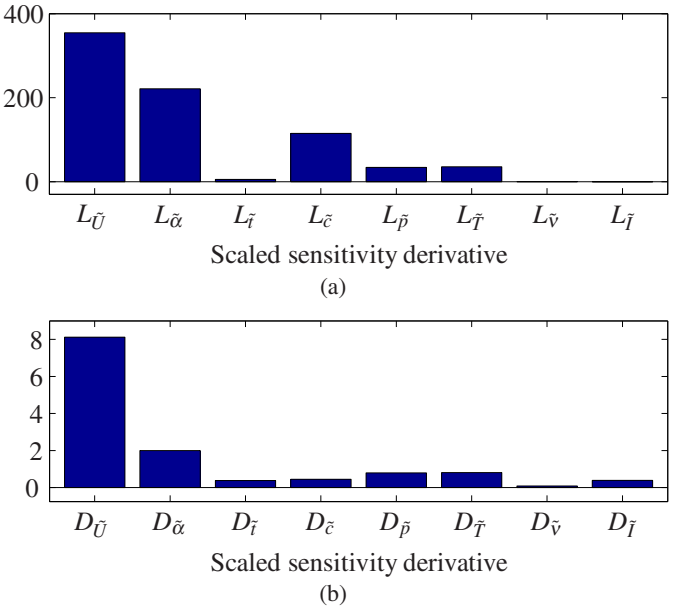

Figure 3: Scaled sensitivity derivatives of the lift L (a) and drag D (b) forces.

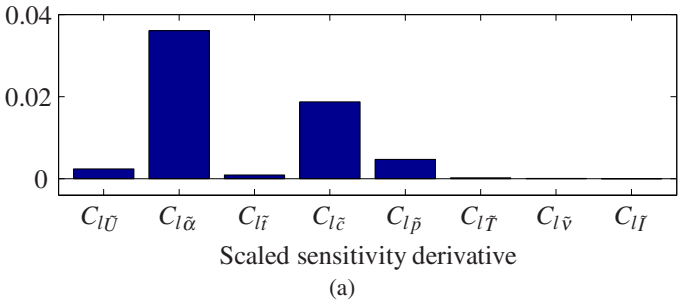

(a)

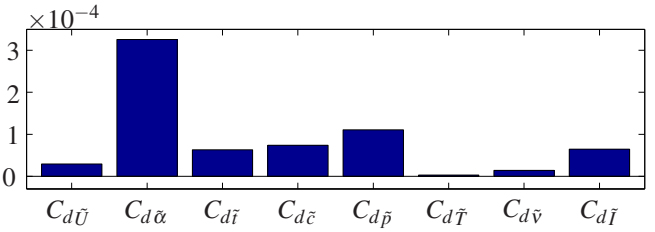

(b)

Figure 4: Scaled sensitivity derivatives of the lift C_l (a) and drag C_d (b) coefficients.

3.2 Step II: Propagating the Probability Distributions

The probability distribution functions of the free stream velocity U, angle of attack α, and camber c are propagated using the Probabilistic Collocation method for p =1,2, and 3, requiring 8, 27, and 64 deterministic computations respectively. The convergence is checked by estimating the error using an approximation of one order higher. The estimated error of the lift force L for a p^{th} order approximation is given by

$$\varepsilon_L = \frac{\sqrt{\frac{1}{N_{p+1}} \sum_{i=1}^{N_{p+1}} w_i \left(L_i^{p+1} - \hat{L}_i \right)^2}}{\frac{1}{N_{p+1}} \sum_{i=1}^{N_{p+1}} \hat{L}_i}, \tag{17}$$

where N_{p+1} is the number of collocation points, L_i^{p+1} are the lift forces for the collocation points, all corresponding to a $(p+1)^{\text{th}}$ order approximation. $\hat{L}_i$ are the estimated lift forces at the collocation points of the $(p+1)^{\text{th}}$ order approximation using a p^{th} order approximation. The resulting convergence of the lift and drag forces are

shown in Fig. 5. To estimate the error of the third order approximation a fourth order computation was performed (requiring 125 deterministic solves). Based on Fig. 5, a first order approximation would be sufficient for this case. However, since it is known that the forces depend quadratically on the free stream velocity, a second order approximation would be appropriate here. Further results are, therefore, obtained from a second order Probabilistic Collocation approximation. So a total of 27 deterministic solves were required for the following results.

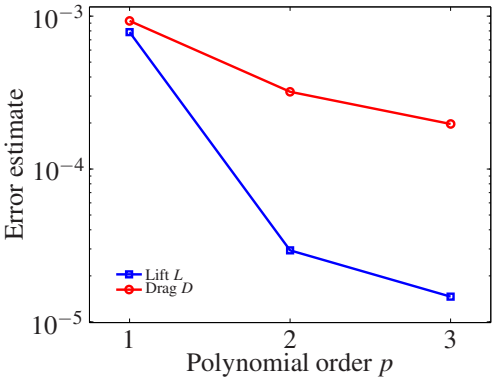

Figure 5: Convergence of the lift and drag forces with respect to the polynomial order.

The statistics of the lift and drag are summarized in Tab. 2. The deterministic values are $L = 3395.763\ N$, $D = 79.41934\ N$, $C_L = 0.5544$, and $C_D = 0.012966$. The difference between deterministic and mean values of the coefficients are less than one count (a lift count is defined as 10^{-3}, and a drag count as 10^{-4}), this difference is negligible. On average the performance of the airfoil remains the same with the assumed uncertainties. The input uncertainties, however, result in possible variations of the output. A good indication for the variability of the output is the coefficient of variation (COV), defined as $COV = \sigma/\mu$. The lift and drag force show a variation of 12.59% and 10.39% respectively. The variation of the lift and drag coefficients of 7.24% and 2.56% is smaller. These variations correspond very well with expected variations based on the sensitivity analysis in section 3.1.

Fig. 6 shows the distribution functions of the lift and drag forces, which look similar to the truncated normal input distribution. This indicates that the propagation is almost linear, although some skewness is introduced. The mean values are the most probable points and points away from the mean have less probability to occur. The distributions of the lift and drag coefficients are shown in Fig. 7, which show a similar picture. The drag coefficient has a small variation, all possible values fall

Table 2: Statistics of the solution resulting from uncertain free stream velocity U, angle of attack α and airfoil camber c using a second order Probabilistic Collocation expansion.

Quantity	Mean μ	Standard deviation σ	Minimal value	Maximal value	Coefficient of variation (COV)
Lift force L $[N]$	3404.991	428.602	1923.069	5408.222	12.59%
Lift coefficient C_L	0.5543	0.0401	0.402108	0.7043135	7.24%
Drag force D $[N]$	79.86150	8.29917	53.74992	113.9887	10.39%
Drag coefficient C_D	0.013004	0.000333	0.012019	0.014354	2.56%

inside an interval of 24 counts. Whereas the interval of all possible values of the lift coefficients covers about 300 counts, which is very large.

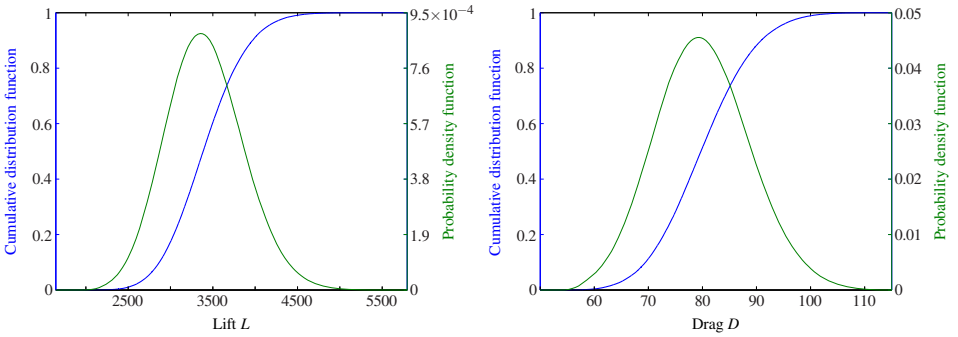

Figure 6: Distribution functions of the lift and drag forces resulting from uncertain U, α, and c using a second order Probabilistic Collocation approximation.

The variations in lift and drag are a direct consequence of variations in the pressure and skinfriction on the surface of the airfoil. Fig. 8 shows the pressure distribution on the surface of the airfoil. The dashed lines indicate the interval which contain 100% of all possible outcomes. The shading presents the probability of the solution, dark blue means a high probability, white is no probability. First Fig. 8(a) shows the relative pressure P/P_0, where P_0 is the free stream pressure. Secondly, Fig. 8(b) shows the pressure coefficient $C_P = (P - P_0)/(\frac{1}{2}\rho U_0^2)$, which is much less affected by the uncertain parameters. The figures show that a large contribution on the uncertainty bounds of the relative pressure is due to the dynamic pressure.

Fig. 9(a) shows the skinfriction on the surface of the airfoil. The variation of the skinfriction is much less than the variation of the pressure, this results in less vari-

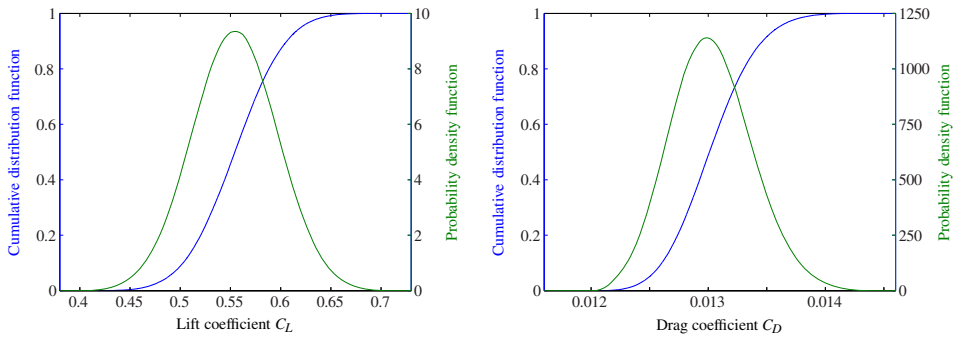

Figure 7: Distribution functions of the lift and drag coefficients resulting from uncertain U, α, and c using a second order Probabilistic Collocation approximation.

ation in drag compared to lift. The skinfriction coefficient $C_f = \tau_w/(\frac{1}{2}\rho U_0^2)$ on the surface is shown in Fig. 9(b), which turns out to be insensitive to the input uncertain parameters. As a result the drag coefficient shows a very low coefficient of variation.

4 Conclusions

A Two-Step approach for efficient uncertainty quantification for computationally intensive problems was presented. The approach starts with a sensitivity analysis based on the scaled sensitivity derivatives of the output of interest with respect to each uncertain parameter. The sensitivity derivative is computed using a first or second order Probabilistic Collocation approximation. The sensitivity analysis is used to identify the most important parameters. When the most important parameters are identified, the probability distribution functions are propagated using higher order Probabilistic Collocation approximations.

The Two-Step approach was applied to a NACA0012 airfoil with 8 uncertain parameters. The parameters were present in the boundary conditions and geometry of the airfoil. Since a single RANS computation runs in the order of 10 CPU hours on an AMD Opteron 2800 MHz processor, it is infeasible to propagated all 8 parameters for orders higher than one. A second order approximation requires already 6561 deterministic computations. Therefore, the Two-Step framework has been applied. The sensitivity analysis identified the importance of each parameter. From the results the velocity U, angle of attack α, and camber c are found to be most important for the output of interest, in this case the lift and drag forces and coefficients of the airfoil. Result show the resulting distribution functions of the

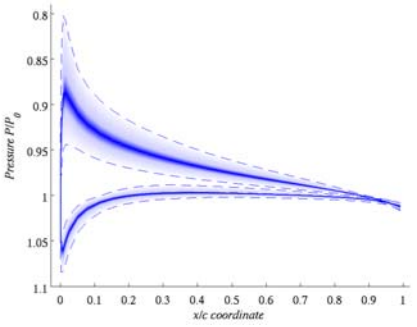

(a) Relative pressure P/P_0

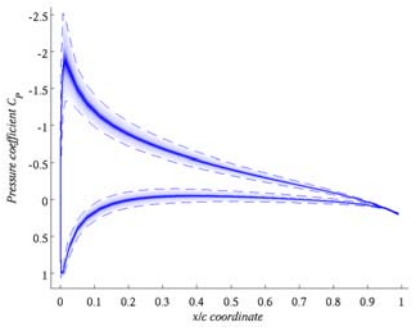

(b) Pressure coefficient C_P

Figure 8: Relative pressure P/P_0 and pressure coefficient C_P on the surface of the airfoil. The dashed lines (--) indicate the interval that covers all possible outcomes. The shaded area indicates the probability of the solution.

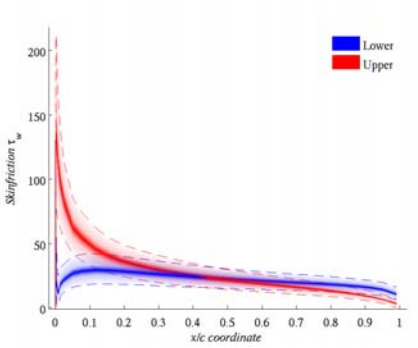

(a) Skinfriction τ_w

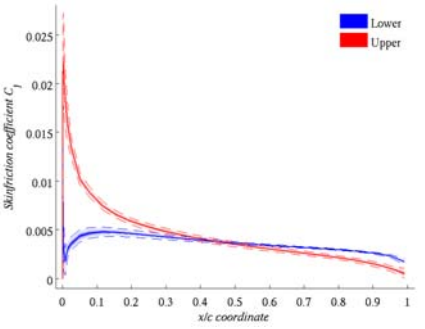

(b) Skinfriction coefficientC_f

Figure 9: Skinfriction τ_w and skinfriction coefficient C_f on the lower (--) and upper (--) surface of the airfoil. The dashed lines indicate the interval that covers all possible outcomes. The shaded area indicates the probability of the solution.

lift and drag forces and coefficients. Furthermore, the effect of the uncertain input parameters on the pressure and skinfriction on the surface of the airfoil are shown. To obtain the final results a total of 44 deterministic computations were required, 17 for the sensitivity analysis and 27 for the second order Probabilistic Collocation computations.

Acknowledgement: The presented work is supported by the NODESIM-CFD project (Non-Deterministic Simulation for CFD based design methodologies); a

collaborative project funded by the European Commission, Research Directorate-General in the 6th Framework Programme, under contract AST5-CT-2006-030959.

References

Babuška, I.; Nobile, F.; Tempone, R. (2007): A stochastic collocation method for elliptic partial differential equations with random input data. vol. 45, no. 3, pp. 1005–1034.

Babuška, I.; Nobile, F.; Zouraris, G. E.; Tempone, R. (2004): Galerkin finite element approximations of stochastic elliptic partial differential equations. vol. 42, no. 2, pp. 800–825.

Ganapathysubramanian, B.; Zabaras, N. (2007): Sparse grid collocation schemes for stochastic natural convection problems. *Journal of Computational Physics*, vol. 225, pp. 652–685.

Gander, M. J.; Karp, A. H. (2001): Stable computation of high order gauss quadrature rules using discretization for measures in radiation transfer. *Journal of Quantitative Spectroscopy Radiative Transfer*, vol. 68, no. 2, pp. 213–223.

Gautschi, W. (2005): Orthogonal polynomials (in matlab). *Journal of Computational and Applied Mathematics*, vol. 178, pp. 215–234.

Ghanem, R. G.; Spanos, P. D. (1991): *Stochastic Finite Elements: A Spectral Approach*. Dover.

Golub, G. H.; Welsch, J. H. (1969): Calculation of gauss quadrature rules. *Mathematics of Computation*, vol. 23, no. 106, pp. 221–230.

Hosder, S.; Walters, R. W.; Perez, R. (2006): A non-intrusive polynomial chaos method for uncertainty propagation in cfd simulations. In *Proceedings of the 44th AIAA Aerospace Sciences Meeting and Exhibit*, Reno. AIAA paper 2006–891.

Loeven, A.; Witteveen, J.; Bijl, H. (2006): Efficient uncertainty quantification using a two-step approach with chaos collocation. In *Proceedings of the ECCOMAS CFD Conference*, Egmond aan Zee.

Loeven, G. J. A.; Sarkar, S.; Witteveen, J. A. S.; Bijl, H. (2007): Dynamic stall flutter analysis with uncertainties using multi-element probabilistic collocation. In *Proceedings of the 9th AIAA Non-Deterministic Approaches Conference*, Waikiki. AIAA paper 2007–1964.

Loeven, G. J. A.; Witteveen, J. A. S.; Bijl, H. (2007): Probabilistic collocation: an efficient non-intrusive approach for arbitrarily distributed parametric uncertainties. In *Proceedings of the 45th AIAA Aerospace Sciences Meeting and Exhibit*, Reno. AIAA paper 2007–317.

Parussini, L.; Pediroda, V. (2007): Fictitious domain with least-squares spectral element method to explore geometric uncertainties by non-intrusive polynomial chaos method. *CMES: Computer Modeling in Engineering & Sciences*, vol. 22, no. 1, pp. 41–63.

Parussini, L.; Pediroda, V. (2008): Investigation of multi geometric uncertainties by different polynomial chaos methodologies using a fictitious domain solver. *CMES: Computer Modeling in Engineering & Sciences*, vol. 23, no. 1, pp. 29–52.

Reagan, M. T.; Najm, H. N.; Ghanem, R. G.; Knio, O. M. (2003): Uncertainty quantification in reacting-flow simulations through non-intrusive spectral projection. *Combustion and Flame*, vol. 132, pp. 545–555.

Sarkar, S.; Witteveen, J. A. S.; Loeven, A.; Bijl, H. (2008): Effect of uncertainty on the bifurcation behavior of pitching airfoil stall flutter. *Journal of Fluids and Structures*.

Tatang, M. A.; Pan, W.; Prinn, R. G.; McRae, G. J. (1997): An efficient method for parametric uncertainty analysis of numerical geophysical models. *Journal of geophysical research*, vol. 102, no. D18, pp. 21925–21932.

Turgeon, E.; Pelletier, D.; Borggaard, J. (2003): Applications of continuous sensitivity equations to flows with temperature-dependent properties. *Numerical Heat Transfer*, vol. 44, pp. 611–624.

Wiener, N. (1938): The homogeneous chaos. *Amer. J. Math.*, vol. 60, no. 4, pp. 897–936.

Xiu, D.; Hesthaven, J. (2005): High order collocation methods for differential equations with random inputs. *SIAM J. Sci. Comput.*, vol. 27, no. 3, pp. 1118–1139.

Xiu, D.; Karniadakis, G. E. (2002): The Wiener-Askey polynomial chaos for stochastic differential equations. *SIAM J. Sci. Comput.*, vol. 24, no. 2, pp. 619–644.

Xiu, D.; Lucor, D.; Su, C. H.; Karniadakis, G. E. (2002): Stochastic modeling of flow-structure interactions using generalized polynomial chaos. *J. Fluids Eng.*, vol. 124, pp. 51–59.